Structural and Electro-Optical Properties of Co-Doped Yttria-Stabilized Zirconia

[a]M. HARTMANOVÁ, [b]F. HANIC, [b]D. TUNEGA, and [b]K. PUTYERA

[a]*Institute of Physics, Slovak Academy of Sciences, SK-842 28 Bratislava*

[b]*Institute of Inorganic Chemistry, Slovak Academy of Sciences, SK-842 36 Bratislava*

Received 17 March 1997

The behaviour of lattice parameter of ZrO_2 + 12 mole % Y_2O_3 as a function of cobaltic oxide addition (0.1—0.5 mass % Co_2O_3) allows to assume the formation of two types of solid solutions, substitutional and interstitial and their mutual coexistence at $w > 0.3$ mass % Co_2O_3. The crystallographic ordering of oxygen sublattice according to this structural model results in the maximum of electrical conductivity observed at ≈ 0.1 mass % Co_2O_3 and the corresponding changes in the Raman spectra and in the shape of infrared modes.

The influence of additive oxides on the structural and electro-optical properties of stabilized zirconia, especially on its ionic conductivity, has been intensively investigated. The special family of oxides added to the stabilized zirconia is that of transition metal oxides. In spite of attention devoted to such systems (*e.g.* [1—7]), the present data are not sufficient to describe their total features.

The purpose of this study is to continue in our investigation of chosen properties of c-ZrO_2 compositions, mainly yttria-stabilized zirconia (YSZ) doped with transition metal oxides [8—13], in this present paper doped with Co_2O_3, and in such way to contribute to the knowledge of these systems.

EXPERIMENTAL

Preparation of samples: YSZ samples with the cobalt dopant were prepared both in the single crystalline and ceramic form: ZrO_2 + 12 mole % Y_2O_3 + w Co_2O_3 (w = 0, 0.1, 0.2, 0.3, and 0.5 mass %).

The single crystals were prepared by the direct inductive melting in the cooling container [14]. The ceramic samples were prepared by means of technology described in [8].

Lattice parameter was evaluated from the indexed powder diffraction data obtained on the Philips 1050 PW diffractometer using CuK_α radiation. α-Alumina (w_r = 1:1) was used as the internal standard.

Density was determined using previously calibrated pycnometer. The distilled water was used as a liquid medium. The air bubbles were removed by reducing pressure. The accuracy of determination was better than 0.05 %.

Microstructure was evaluated from photomicrographs prepared for the ceramic samples mechanically polished by diamond paste and coated with a thin layer of gold to prevent their charging under impact of the electron beam in the scanning electron microscope Tesla BS 300 (acceleration voltage 25 kV). The grain size was measured according to *Mendelson* [15].

Electrical conductivity has been investigated in the frequency range 10—10^5 Hz at the temperature 199—342 °C in the air. The conductance and the capacitance were measured by means of GR Capacitance Bridge 1616. The temperature was stabilized by Chinoterm 10 A digital temperature controller with the accuracy of ± 0.5 °C. The platinum paste electrodes were applied to the entire circular faces of discs.

IR reflectance spectra were obtained using Perkin—Elmer 983G spectrophotometer equipped with specular attachment. The reflectance measurements were made at near normal-incidence arrangement in the spectral range of 180—1000 cm^{-1}.

Raman spectra: The measurements of unpolarized Raman spectra were carried out on Jeol JRS-S1 spectrophotometer (double-grating monochromator and photon-counting system). The 640 nm line of the He-Ne laser was used as exciting radiation. All spectra were measured in the right-angle scattering geometry.

Both IR reflectance and Raman spectra were obtained at room temperature.

RESULTS AND DISCUSSION

Structural Data of Investigated Samples

The structural data of investigated samples as the function of Co_2O_3 concentration are summarized in Table 1.

Table 1. Structural Data (Experimental and Calculated) of the System ZrO_2 + 12 mole % Y_2O_3 + w mass % Co_2O_3: Lattice Parameter a, Unit Cell Volume V, Molar Mass M, Density ρ, Porosity η, and Average Grain Size $\overline{D}$

w	a_{exp}	V	a_{calc}	M	ρ_{calc}	ρ_{exp}	η	$\overline{D}$
mass %	nm	10^{-3} nm^3	nm	g mol^{-1}	g cm^{-3}	g cm^{-3}	%	μm
0.0	0.51510(2)	136.671	0.515414	484.887	5.878	5.197 ± 0.002	11.58	9.842 ± 0.301
0.1	0.514623(9)	136.291	0.515337	484.661	5.885	5.208 ± 0.002	11.52	11.927 ± 0.246
0.2	0.514531(9)	136.218	0.515259	484.523	5.884	5.209 ± 0.002	11.48	9.609 ± 0.229
0.3	0.515171(9)	136.727	0.515181	484.214	5.876	5.233 ± 0.002	10.95	11.259 ± 0.317
0.5	0.515370(7)	136.886	0.515379	483.766	5.886	5.284 ± 0.002	10.24	15.608 ± 0.589

The observed dependence of the lattice parameter a_{exp} of YSZ on the Co_2O_3 concentration allows to assume the formation of two types of solid solutions within the investigated cobaltic oxide concentration range in the system ZrO_2—Y_2O_3—Co_2O_3. The tendency of lattice parameter a_{exp} to decrease with the increasing cobaltic oxide concentration up to 0.2 mass % corresponds to the formation of the substitutional solid solution, since the Zr^{4+} cation in the fluorite type structure of YSZ is replaced with the cobalt cation with the smaller effective cation radius. The lower used concentrations of added impurity (0.1—0.3 mass %) enter the substitutional positions. The highest used Co_2O_3 amount (0.5 mass %) occupies simultaneously both substitutional and interstitial positions. The distribution of cobalt cations between substitutional (s) and interstitial (i) sites is in agreement with the formula [9]

$$(Zr^{4+}_{0.806-s}Y^{3+}_{0.194}\ Co^{3+}_s)(Co^{3+}_i)O^{2-}_{1.903+(3i-s)/2} \quad (1)$$

where the total number f of cobalt cations is

$$f = s + i \quad (2)$$

The values of s and i were evaluated from the comparison of observed (a_{exp}) and calculated (a_{calc}) unit cell parameters given by the relationship

$$a_{calc} = 4/\sqrt{3}\{(0.806 - s)\cdot r(Zr^{4+}) + 0.194\cdot r(Y^{3+}) + s\cdot r(Co^{3+})[0.951 + (3i - s)/4]^{1/3}\cdot r(O^{2-})\} \quad (3)$$

where $r(X)$ is the effective ionic radius of ion X.

The agreement between calculated, a_{calc}, and observed, a_{exp}, lattice parameters was obtained by proper optimization of i and s values. The relevant values of f corresponding to mass % Co_2O_3 were: 0.00146, 0.00292, 0.00439, and 0.00732. The ionic radii of elements in 8(and 4)-fold coordination were used according to [16]

$^{VIII}r(Zr^{4+}) = 0.084$ nm, $^{VIII}r(Y^{3+}) = 0.1019$ nm, $^{IV}r(O^{2-}) = 0.138$ nm

Taking into account the known property of cobalt to change the valence state (*i.e.* III → II) [17], then a part of cobalt cations is present as Co^{2+} with ionic radius $^{VIII}r(Co^{2+}) = 0.0855$ nm. In such way, the agreement between a_{exp} and a_{calc} especially for the highest cobalt concentration is found to be very good.

The increase in impurity concentration is accompanied also by a slight decrease of porosity η and increase of average grain size $\overline{D}$, as it can be seen in Table 1. The porosity η of ceramic samples was calculated using the relation: $\eta = [(\rho_{calc} - \rho_{exp})/\rho_{calc}] \times 100$ %.

Electrical Conductivity

The bulk conductivity σ_{bulk} as a function of impurity content has maximum at ≈ 0.1 mass % Co_2O_3 as it can be seen in Table 2, where the investigated electrical characteristics of the samples are summarized. The bulk conductivity values have been fitted to the Arrhenius-type expression

$$\sigma_{bulk} = A\cdot\exp(E/kT) \quad (4)$$

where A is the preexponential factor, E is the activation energy, and kT is the Boltzmann factor.

The observed dependence of σ_{bulk} on the concentration of cobalt dopant can be explained by the proposed structural model consisting in the formation of two types of solid solutions. The cobalt dopant enters the parent crystals in two ways. Primarily, the Co^{3+} ions substitute Zr^{4+} ions in the crystal structure, *i.e.*

$$Co_2O_3 \rightarrow 2Co'_{Zr} + V_O^{\cdot\cdot} + 3O_O \quad (5)$$

where Co_{Zr} is Co^{3+} ion in Zr^{4+} site and V_O is an oxygen vacancy. The effect of the smaller cobalt cation ($^{VIII}r(Co^{3+}) = 0.07117$ nm) substituting for the larger zirconium cation ($^{VIII}r(Zr^{4+}) = 0.084$ nm) causes the lattice spacing contraction up to 0.2 mass % Co_2O_3 concentration. A part of cobalt cations, above the impurity concentration 0.3 mass %, enters the YSZ samples interstitially, *i.e.*

$$Co_2O_3 + 3V_O^{\cdot\cdot} \rightarrow 2Co_i^{\cdot\cdot\cdot} + 3O_O \quad (6)$$

Table 2. Electrical Characteristics of YSZ + w mass % Co_2O_3: Bulk Electrical Conductivity σ_{bulk}, Activation Energy E, and Preexponential Factor A at $\theta = 275\,°C$

w	σ_{bulk}	E	A
mass %	$10^{-5}\ \Omega^{-1}\ m^{-1}$	eV	$10^{6}\ \Omega^{-1}\ m^{-1}$
0.0	2.41	1.18 ± 0.01	1.85 ± 0.02
0.1	4.00	1.20 ± 0.01	2.76 ± 0.05
0.2	3.47	1.18 ± 0.02	2.57 ± 0.03
0.3	2.80	1.20 ± 0.01	3.22 ± 0.05
0.5	2.62	1.19 ± 0.01	2.38 ± 0.03

where Co_i is an interstitial Co^{3+} ion. The increase of lattice parameter a_{exp} *vs.* w (dissolved Co_2O_3 at $w >$ 0.3 mass %) indicates that the cobalt ions enter the zirconia system in both ways – substitutionally and interstitially ($s = 0.00472$, $i = 0.00260$) under the applied conditions. At the same time, a part of cobalt cations is reduced from valence state III to II. The concentration and structural changes influence the properties of the oxygen sublattice resulting in an observed conductivity maximum of the samples.

Optical Spectra

The crystal structure of stabilized c-ZrO_2 is of disordered *fcc* fluorite type.

While the cation sublattice possesses a perfect cubic structure (Zr^{4+} ions are randomly replaced by Y^{3+} ions), the oxygen sublattice is disordered due to vacancies. This fact means that the c-ZrO_2 loses generally the translation symmetry. Therefore, the translational disorder causes breakdown of $\boldsymbol{k} = 0$ selection rule for Raman scattering and IR absorption in the crystal. This fact is reflected both in Raman and IR spectra. While for a perfect *fcc* crystal only one mode with the F_{2g} symmetry is active in Raman spectra from the first-order Raman effect, in Raman spectra of disordered *fcc* structures (*e.g.* [18]) several broad Raman active modes were observed. The dominant band in these spectra at $\tilde{\nu} \approx 600\ cm^{-1}$ was assigned to original F_{2g} band in the perfect *fcc* crystal. Its broadening and structure are caused by the mentioned breakdown of selection rule. From polarized and temperature-dependent measurements [18] it was found that the new additional broad Raman bands in regions below 500 cm^{-1} are caused by defects in anion oxygen sublattice and are called defect-induced Raman bands. The structure and the intensity of these modes will depend on the structure of defects in the crystals [18, 19].

The Raman spectra of pure YSZ and YSZ doped with Co_2O_3 are compared in Fig. 1. The structure of defect-induced modes in YSZ + Co_2O_3 crystals is similar to that of undoped YSZ. The observed decrease in the intensities of defect-induced modes of YSZ + w Co_2O_3 up to the composition of YSZ + 0.2 mass % Co_2O_3 is in agreement with the crystallographic ordering of oxygen sublattice under the assumed formation of substitutional and interstitial solid solutions.

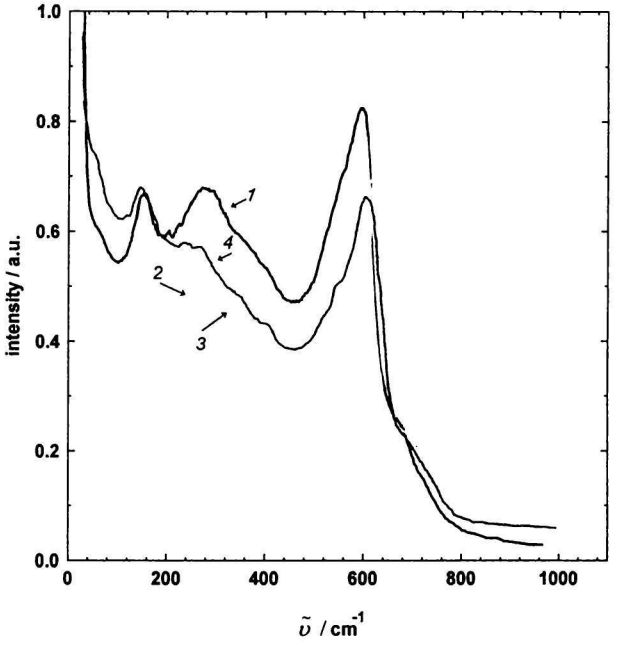

Fig. 1. Raman spectra of YSZ doped with Co_2O_3. *1.* ZrO_2—12 mole % Y_2O_3; *2.* ZrO_2—12 mole % Y_2O_3—0.1 mass % Co_2O_3; *3.* ZrO_2—12 mole % Y_2O_3—0.2 mass % Co_2O_3; *4.* ZrO_2—12 mole % Y_2O_3—0.3 mass % Co_2O_3.

The structural defects in the oxygen sublattice have the same effect on the IR reflection modes as they have on the Raman spectra. The crystallographic ordering mainly influences the shape of the reflectance spectra, which can be seen in Fig. 2. The certain broadening of the "Restrahlen" band at $\tilde{\nu} \approx 470\ cm^{-1}$ with increasing Co concentration and the increase of smaller shoulder at 615 cm^{-1} are evident.

CONCLUSION

The presence of cobalt dopant in YSZ in the mass fraction range of 0.1—0.5 % Co_2O_3 results in:

– the decrease of the observed lattice parameter a_{exp} as a function of cobalt dopant up to 0.2 mass % Co_2O_3 then followed by the increase of lattice param-

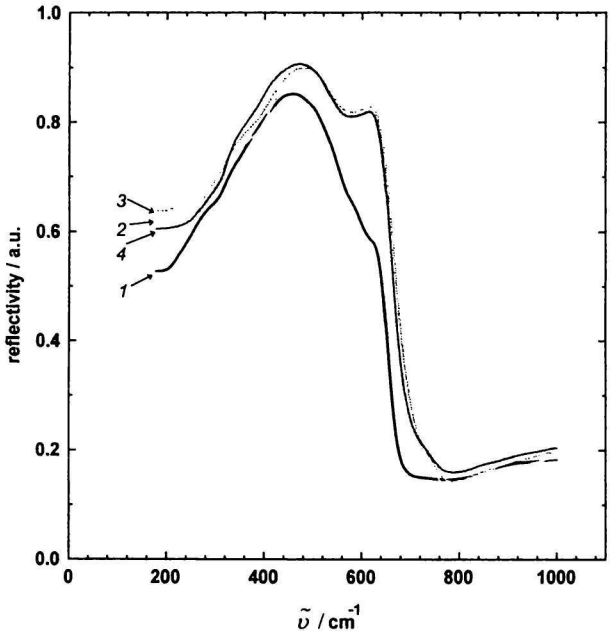

Fig. 2. Reflectivity spectra of YSZ doped with Co_2O_3. *1.* ZrO_2—12 mole % Y_2O_3; *2.* ZrO_2—12 mole % Y_2O_3—0.1 mass % Co_2O_3; *3.* ZrO_2—12 mole % Y_2O_3—0.2 mass % Co_2O_3; *4.* ZrO_2—12 mole % Y_2O_3—0.3 mass % Co_2O_3.

eter with the next increasing of the dopant content. This fact can be compared with the theoretical values a_{calc}. The comparison allows to assume formation of substitutional solid solution, but a mixed solid solution can be expected for the w value 0.5 mass % Co_2O_3 with $s = 0.00472$ and $i = 0.00260$. This gives the best comparable value with the observed lattice parameter a_{exp} ($a_{exp} = 0.515370$ nm, $a_{calc} = 0.515379$ nm);

– the crystallographic ordering of oxygen sublattice according to the proposed structural model that caused the maximum of electrical conductivity at $w \approx 0.1$ mass % Co_2O_3 and the corresponding changes in the Raman and reflection IR spectra.

Acknowledgements. This work was supported in part by the Research Grants No. 2/1004/96, 2/1172/96, and 2/1165/96 of the Slovak Grant Agency.

REFERENCES

1. Kawada, T., Sakai, N., Yokokawa, H., and Dokiya, M., *Solid State Ionics 53—56*, 418 (1992).
2. Liou, S. S. and Worell, W. L., Proc. First Int. Symp. on Solid Oxide Fuel Cells, *Electrochem. Soc. Proc. 89—91*, 81 (1989).
3. Schouler, E. J. L. and Kleitz, M., *J. Electrochem. Soc. 134*, 1047 (1987).
4. Matsui, N., *Denki Kagaku 58*, 716 (1990).
5. Van Hassel, B. A. and Burggraaf, A. J., *J. Appl. Phys., A 53*, 155 (1991).
6. Gilderman, V. K., Niuimin, A. D., Palguev, S. F., and Toporov, Yu. S., *Elektrokhimiya 12*, 1585 (1976).
7. Wilhelm, R. W. and Howarth, D. S., Jr., *Ceram. Bull. 58*, 228 (1979).
8. Hartmanová, M., Machovič, L., Koller, A., Hanic, F., and Mišanik, B., *Solid State Ionics 14*, 93 (1984).
9. Hanic, F., Hartmanová, M., Urusovskaya, A. A., Knab, G. G., Iofis, N. A., and Zyryanova, I. L., *Solid State Ionics 36*, 197 (1989).
10. Spišiak, J., Hartmanová, M., Knab, G. G., and Krcho, S., *J. Eur. Ceram. Soc. 11*, 509 (1993).
11. Knab, G. G., Konstantinova, A. F., Ulukhanov, I. T., Hartmanová, M., Hanic, F., Urusovskaya, A. A., Iofis, N. A., and Zyryanova, I. L., *Kristallografiya 35*, 923 (1990).
12. Hartmanová, M., Poulsen, F. W., Hanic, F., Urusovskaya, A. A., Putyera, K., Tunega, D., and Oreshnikova, T. V., *J. Mater. Sci. 29*, 2152 (1994).
13. Norby, T. and Hartmanová, M., *Solid State Ionics 67*, 57 (1993).
14. Aleksandrov, V. I., Osiko, V. V., Prokhorov, A. M., and Tatarintsev, V. M., *Usp. Khim. 47*, 385 (1978).
15. Mendelson, M. I., *J. Am. Ceram. Soc. 52*, 443 (1969).
16. Shannon, R. D., *Acta Crystallogr., A 32*, 75 (1976).
17. Aleksandrov, V. I., Batygov, S. Kh., Vishniakova, M. A., Voronko, Yu. K., Kalabukhova, V. F., Lavriskhev, S. V., Lomonova, E. E., Myzina, V. A., and Osiko, V. V., *Fiz. Tverd. Tela 26*, 1313 (1984).
18. Ishigame, M. and Yoshida, E., *Solid State Ionics 24*, 211 (1987).
19. Liu, D. W., Perry, C. H., and Ingel, R. P., *J. Appl. Phys. 64*, 1413 (1988).

Translated by M. Hartmanová